

Determination of the blocking temperature of magnetic nanoparticles: The good, the bad and the ugly

P. Mendoza Zélis,^{1,2, a)} I.J. Bruvera,^{1, b)} M.Pilar Calatayud,^{3,4} G.F. Goya,^{3,4} and F.H. Sánchez¹

¹⁾IFLP-CCT- La Plata-CONICET and Departamento de Física, Facultad de Ciencias Exactas, C. C. 67, Universidad Nacional de La Plata, 1900 La Plata, Argentina

²⁾Departamento de Ciencias Básicas, Facultad de Ingeniería, Universidad Nacional de La Plata, 1900 La Plata, Argentina

³⁾Aragon Institute of Nanoscience (INA), University of Zaragoza, 50018, Spain

⁴⁾Condensed Matter Physics Department, Science Faculty, University of Zaragoza, 50009, Spain

In a magnetization vs. temperature (M vs. T) experiment, the blocking region of a magnetic nanoparticle (MNP) assembly is the interval of T values where the system begins to respond to an applied magnetic field H when heating the sample from the lower reachable temperature. The location of this region is determined by the anisotropy energy barrier depending on the applied field H , the volume V , the magnetic anisotropy constant K of the MNPs and the observing time of the technique. In the general case of a polysized sample, a representative blocking temperature value T_B can be estimated from ZFC-FC experiments as a way to determine the effective anisotropy constant.

In this work, a numerical solved Stoner-Wolfarth two level model with thermal agitation is used to simulate ZFC-FC curves of monosized and polysized samples and to determine the best method for obtaining a representative T_B value of polysized samples. The results corroborate a technique based on the T derivative of the difference between ZFC and FC curves proposed by Micha *et al* (the good) and demonstrate its relation with two alternative methods: the ZFC maximum (the bad) and inflection point (the ugly). The derivative method is then applied to experimental data, obtaining the T_B distribution of a polysized Fe_3O_4 MNP sample suspended in hexane with an excellent agreement with TEM characterization.

I. INTRODUCTION

Magnetic nanoparticles (MNPs) are been extensively studied due to their multiple applications in technology¹ and biomedicine^{2,3}. Particles with sizes in the range $[5, 100]nm$ ⁴ present a magnetic behaviour determined by its volume, shape and composition, matrix viscosity and temperature, among other factors. In the simplest (however very useful) model, the MNPs of volume V and saturation magnetization M_s are considered as almost spherical ellipsoids with a permanent moment $m = M_s V$ and a preferential magnetization axis (easy axis) in which the anisotropy energy $E_K = KV \sin^2[\delta]$ is minimum, being K the effective anisotropy density constant and δ the angle between m and the easy axis. If the MNPs are fixed in the matrix and separated one from each other by a distance $d > 3V^{1/3}$, dipolar interactions can be neglected⁵ and the energy of the system can be expressed as the sum of the anisotropy energy and the Zeeman energy $E_H = -mH \cos[\theta]$:

$$E = E_K + E_H, \quad (1)$$

with θ the angle between m and H (fig. 1). This configuration is usually called Stoner-Wolfarth system since the publication of a work⁶ in which the authors perform

a numerical calculation of the M vs. H curves of ordered systems with different orientations *i.e.* systems of identical MNPs with a single value of ϕ , and the M vs. H curve of a disordered system *i.e.* with a uniform distribution of ϕ values. Since no thermal agitation was considered by Stoner and Wolfarth, their calculations were made just finding the positions θ_i of the minima of equation 1 for each value of H .

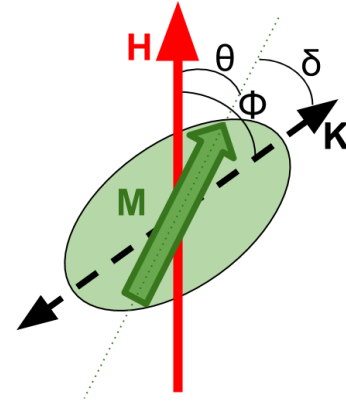


FIG. 1. MNP model. The energy is determined by the angle δ between the magnetization M and the field H , and the angle θ between M and the easy axis K . For calculation simplicity the angle $\phi = \theta + \delta$ between K and H is used.

^{a)}Electronic mail: pmendoza@fisica.unlp.edu.ar

^{b)}Electronic mail: bruvera@fisica.unlp.edu.ar

In order to calculate the temperature dependence of the magnetic response for MNPs systems, it is necessary to consider the effect of thermal fluctuations that

allow transitions between stable configurations. Doing so, it is possible to simulate M vs. T experiments as the extensively performed Zero Field Cooling-Field Cooling (ZFC-FC) routine. In this kind of experiments, a sample is cooled from a temperature where all particles show superparamagnetic behaviour to the lowest reachable temperature (usually around $3K$), then, a small constant field usually lower than $8kA/m$ is applied, and the sample is heated to a temperature high enough to observe an initial growth and subsequent decrease in magnetization, i.e. were the sample show again superparamagnetic behaviour. The sample is then cooled again to the lowest temperature with the constant field still applied.

In the ideal case of a monosized, non interacting MNPs sample; a narrow temperature region should exist in which the system performs a transition between irreversible and reversible regimes. When heating with applied field, the thermal energy kT is initially much smaller than the anisotropy barrier KV so the magnetization remains null. Due to the exponential dependence of the Néel relaxation time with temperature⁷, when $kT \sim KV$, the magnetization grows rapidly until its thermodynamic equilibrium value, defining the aforementioned transition region. The Blocking Temperature T_B can be considered as the inflection point of this growing and its experimental determination is an important goal of the MNPs characterization.

Real samples always present a size dispersion, usually reasonably well described by a log-normal distribution. Different particle size implies different anisotropy barrier KV and therefore a different T_B for each size fraction, so, in real ZFC-FC experiments, the blocking region is wide and the representative T_B value is not well defined. There are several different criteria used to define a representative T_B from ZFC-FC data of polysized samples. Some authors maintain the inflexion point (IP) criterion⁸ while others report the maximum ZFC magnetization temperature (MAX)^{9,10}, being all this criteria still in discussion¹¹. In an alternative approach, Micha *et al.*¹² propose a method in which the T_B distribution is obtained from the T derivative of the difference between ZFC and FC curves. An approximated theoretical justification for this method was presented by Mamiya *et al.*¹³.

In this work, a SW model with thermal agitation is applied to obtain the temporal dependence of the magnetization $M(t)$ for an ordered system of identical MNPs in a similar way to previous works of Lu¹⁴, Usov¹⁵ and Carrey¹⁶. Temperature dependence $dM(T)/dT$ is then obtained in order to numerically simulate the ZFC-FC curves. In contrast to the method implemented by Usov¹⁷ where a stair-step approximation for the time evolution of the temperature was used, we consider a continuous time evolution. Finally, an ordered polysize system response is simulated by linear combination of the monosize curves weighted by a discrete log-normal distribution.

The validity of the method proposed by Micha *et al*

was verified by comparing the T derivative of this ZFC-FC curve with the T_B distribution obtained from the inflection points of each volume of the distribution. The resultant mean blocking temperature value $\langle T_B \rangle$ is then compared, for several volume distributions, with the commonly used criteria for a representative T_B : the inflection point temperature IP and the maximum MAX of the ZFC curve.

Additionally, Micha's method is tested with experimental data of a magnetite MNPs frozen ferrofluid suspended in hexane comparing the obtained T_B distribution with the one calculated from the TEM size information. In order to obtain an ordered system, the ferrofluid was frozen while a large constant was field applied.

II. MODEL

A SW-like model with thermal agitation and zero width energy minima approximation was developed in order to obtain ZFC-FC curves of fixed MNPs with size dispersion. Only the simplest case of an ordered system was considered, with all the MNPs oriented (easy axis orientation) in the direction of the field. This situation can be achieved experimentally by freezing a ferrofluid sample under a sufficiently strong applied field ($\sim 7T$).

A. Magnetization vs. time equation

For a system of identical, fixed, non interacting MNPs of volume V , anisotropy constant K and saturation magnetization M_s , with their anisotropy axes parallel to an external field H , the energy can be expressed as the sum of the anisotropy energy E_k and the Zeeman energy E_h ⁶:

$$\begin{aligned} E &= E_k + E_h = KV \sin(\theta)^2 - \mu_0 M_s V \cos(\theta) \\ &= KV \left(\sin(\theta)^2 - 2h \cos(\theta) \right), \end{aligned} \quad (2)$$

being $h = H/H_k$ and $H_k = \mu_0 M_s / 2K$.

In the range $\theta = [0, 2\pi]$, this energy landscape presents two minima, of $E(0) = -2KV_h$ and $E(\pi) = 2KV_h$ and a maximum of $E(\arccos(-h)) = KV \left(1 + h^2 \right)$ (fig. 2).

The frequency of thermal inversions between minima i and j is the inverse of the Néel relaxation time^{18,19}:

$$f_{ij} = f_0 e^{D_{ij}/(kT)} \quad (3)$$

with f_0 the "intrinsic frequency", times the Boltzman "success probability" depending on the ratio between thermal energy kT and barrier height D_{ij} . The barrier between minima is symmetric for $h = 0$ with $D_{du} = D_{ud} = KV$ (naming u and d to $\theta = 0$ and $\theta = \pi$ directions respectively) and smaller for inversion to the field

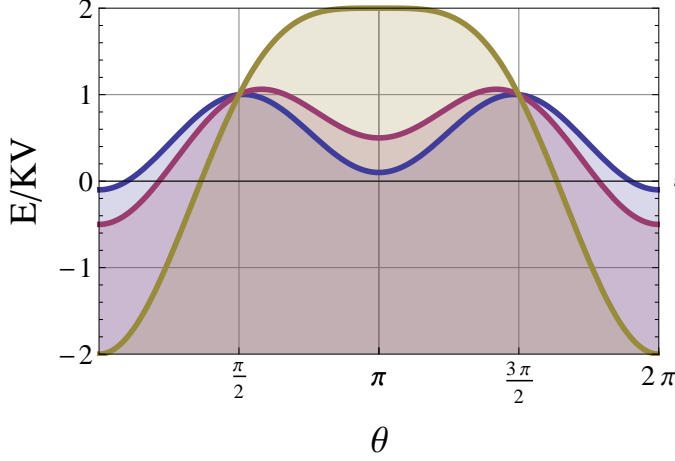


FIG. 2. Energy landscapes as a function of theta for a fixed MNP under a magnetic field at $\theta = 0$. Each color stands for a different value of the reduced field factor $2h$. Blue: $2h = 0.1$, purple: $2h = 0.5$, gold: $2h = 2$.

direction otherwise:

$$\begin{aligned}\Delta_{ud} &= E(\arccos(-h)) - E(\pi) = KV \left(1 + h\right)^2 \\ \Delta_{du} &= E(\arccos(-h)) - E(0) = KV \left(1 - h\right)^2\end{aligned}\quad (4)$$

It is a good approximation to consider the same f_0 value for both frequencies²⁰.

Sample magnetization M in the direction of the applied field can be expressed in terms of saturation magnetization M_s and the number of particles per unit volume magnetized in each direction N_u and N_d :

$$M = (N_u - N_d) M_s / N = M_s \left(2N_u / N - 1\right), \quad (5)$$

with N the total number of particles per unit volume. So the time derivative of the magnetization can be written in terms of the population variation which is equal to the actual population times the inversion probability to each direction

$$\frac{dM}{dt} = 2 \frac{M_s}{N} \frac{dN_u}{dt}. \quad (6)$$

$$\frac{dN_u}{dt} = -\frac{dN_d}{dt} = f_{d \rightarrow u} N_d - f_{u \rightarrow d} N_u. \quad (7)$$

so the time derivative of the relative magnetization m is determined by the transcendental equation

$$\frac{dm}{dt} = 2f_0 e^{-C(1+h^2)} \{\sinh(2Ch) - m \cosh(2Ch)\}. \quad (8)$$

where $C = KV/kT$.

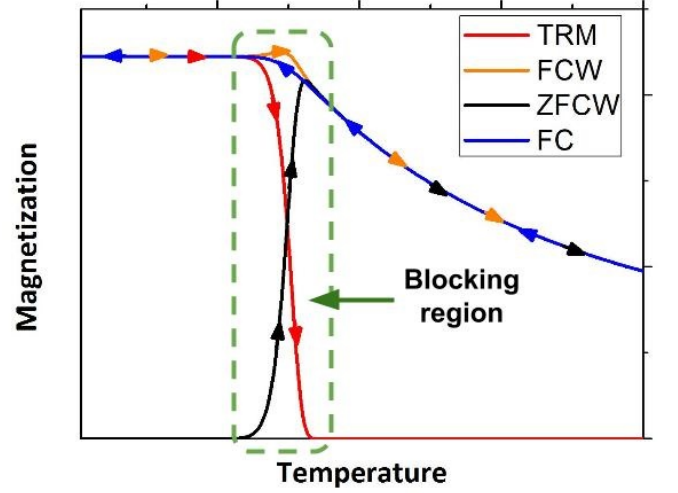


FIG. 3. Simulation result for an ordered assembly of MNPs. The system is first cooled with zero field applied from a high temperature where all particles show superparamagnetic behaviour (ZFC, no showed), then, the field is turned on and the system is heated beyond the blocking region (ZFCW). Maintaining the applied field, the system is cooled (FC). The final heating can be performed with (FCW) or without applied field (TRM).

B. Magnetization vs. Temperature equation: ZFC-FC simulation

Temperature dependence of the magnetization can be obtained from 8 via the equation

$$\frac{dm}{dT} = \frac{dm}{dt} \frac{dt}{dT}. \quad (9)$$

For a linear temperature variation $T(t) = Bt + T_0$, the magnetization derivative is

$$\frac{dm}{dT} = \frac{1}{B} \frac{dm}{dt} = \frac{2f_0}{B} e^{-C(1+h^2)} \{\sinh(2Ch) - m \cosh(2Ch)\} \quad (10)$$

Solving this equation by numerical methods it is possible to simulate a ZFC-FC experiment for a monosize sample. A Matlab script based on the ODE15s²¹ function was developed. An example of the result for a monosize assembly of ordered MNPs is shown in figure 3. Line colours stand for different parts of the routine.

During the warming after zero field cooling (ZFCW for this chapter, usually called just ZFC), the exponential dependence of the inversion frequency with temperature in equation 3 determines a narrow “blocking region” wherein the MNPs, which were “blocked” at low temperature begin to respond to the field. Magnetization grows with temperature since the applied field has decreased the energy barrier for $\theta = \pi$ to $\theta = 0$ inversion. The magnetization increasing reverts when thermal energy is

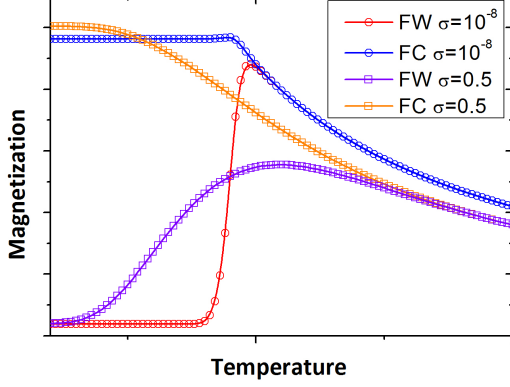


FIG. 4. Comparison between ZFC-FC simulations for small ($\sigma = 10^{-8}$) and large ($\sigma = 0.5$) dispersion systems.

much higher than the barrier, so the difference between inversion frequencies in each direction tends to disappear. The blocking temperature T_B of the system is then defined as the inflection point of the magnetization growing when heating.

When the system is cooled again (FC), magnetization grows monotonically while the barrier height difference between inversions becomes increasingly significant against thermal energy. This growth stops when thermal energy becomes too low for inversions to occur within the experimental window time. If the system is then heated maintaining the applied field (FCW), magnetization values are the same than FC except for the blocking region where there is a small increase due to the assembly getting closer to the equilibrium state. If the final warming is done with no applied field (Thermal Remanent Magnetism, TRM), magnetization drops to zero in the blocking region when thermal energy is enough for the wells populations to equilibrate.

The magnetization values M_p for a polysized sample are obtained by linear addition of the M_{V_i} values for each contemplated size V_i , weighted by the corresponding volume and log-normal distribution $LnN(V_i)$ value:

$$M_p(T) = \frac{\sum_{i=1}^N M_{V_i}(T) V_i LnN(V)}{\sum_{i=1}^N V_i LnN(V)}, \quad (11)$$

The $V_i LnN(V_i)$ product stands for the relative volume distribution.

Figure 4 shows the comparison between ZFC-FC simulations for samples with different size dispersion expressed as the scale parameter σ of the log-normal number distribution. A much wider transition region can be seen for the bigger dispersion so the different aforementioned criteria would define very separated values for a representative T_B .

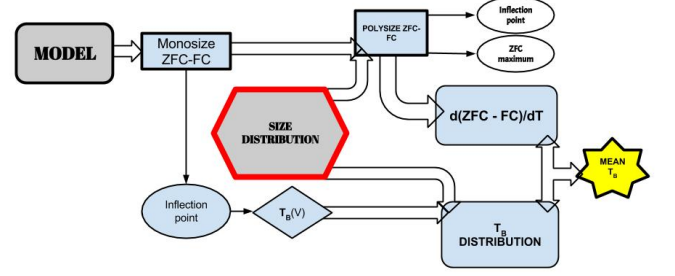


FIG. 5. Scheme of the method verification. Monosize ZFC-FC curves are simulated from the $dM(T)/dT$ equations of the model. In one path, T_B for every particle size is calculated as the IP of the monosize ZFC curve. In the other path, a polysize ZFC-FC curve is simulated by linear addition of the monosize values. Then the T derivative of the difference ZFC-FC is calculated.

III. BLOCKING TEMPERATURE DETERMINATION

A. Micha's method verification

In order to verify Micha's method, several polysize ZFC-FC experiments were simulated using different parameter sets varying σ and the mean radius. For each one of the used sets, the T derivative of the ZFC-FC difference was calculated. Then, the T_B distribution was obtained from the monosize curves that were added to construct the polysize simulation in equation 11: a ZFC curve was calculated for each class of the size distribution so each T_B class comes from a volume class, maintaining the same relative height. Also IP and MAX values of the polysize ZFC curve were calculated and compared with the mean value $\langle T_B \rangle$ of the distribution in each simulation (fig. 5).

In all cases, the T_B distribution and the ZFC-FC derivative are identical. Figure 6 shows the results for the simulation with 4.5 nm mean radius, $\sigma = 0.5$, $16 kJ/m^3$ anisotropy constant and a $4 K/min$ heating rate.

Also, for a set of ZFC-FC curves calculated with the same mean volume, saturation magnetization, heating rate and anisotropy constant, by increasing scale parameter σ , $\langle T_B \rangle$ stays constant while the polysize curve IP shifts to smaller temperatures and MAX shifts in opposite direction. Figure 7 shows the results for 4.5 nm mean radius, $16 kJ/m^3$ anisotropy constant, $4 K/min$ heating rate and $\sigma = [0.1, 0.6]$.

This behaviour is the same in the hole studied size range. By normalizing IP values by the T_B mean, all points fall in the same curve as shown in figure 8 while the variation for MAX is small.

Varying the heating rate and K does not affect the relation $IP/\langle T_B \rangle$. Meanwhile, the $MAX/\langle T_B \rangle$ ratio changes strongly in the range $[0.04; 400] K/min$ and noticeably in the range $[1; 10] K/min$ and also depends on the K value. Figure 9 shows the results of varying

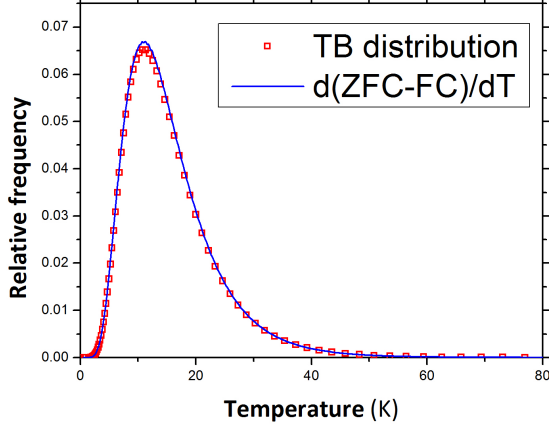


FIG. 6. Comparison between the T_B distribution obtained directly from the size distribution used in the simulation and the derivative $d(\text{ZFC-FC})/dT$ of the simulated curves.

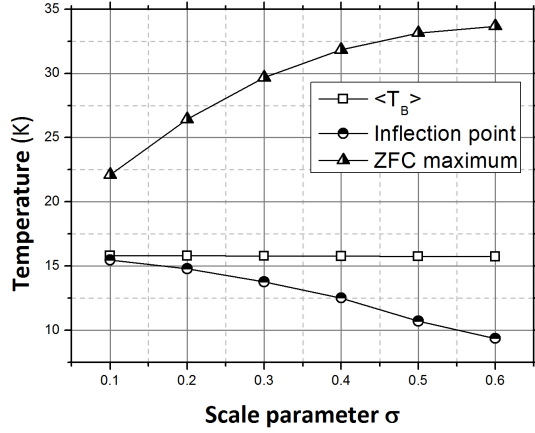


FIG. 7. Values of T_B mean, MAX and IP of the simulated curves as a function of the scale parameter σ for 4.5nm mean radius, $16\text{kJ}/\text{m}^3$ anisotropy constant and $4\text{K}/\text{min}$ heating rate.

the heating rate for $R_m = 10\text{nm}$, $K = 16\text{kJ}/\text{m}^3$ and $M_s = 281\text{kA}/\text{m}$.

Figure 10 shows a parabolic fit over the $IP / \langle T_B \rangle$ values obtained for all the simulations. The curve is universal with small fluctuations due to numeric resolution. The obtained polynomial with fitting errors is $\frac{IP}{\langle T_B \rangle}(\sigma) = 1.00(2) - 0.21(2)\sigma - 0.79(2)\sigma^2$.

B. Experimental application

The Micha's analysis was conducted on ZFC-FC measurements of a FF of magnetite MNPs suspended in hexane with a concentration of $12(1)\text{g}/\text{L}$. TEM images were

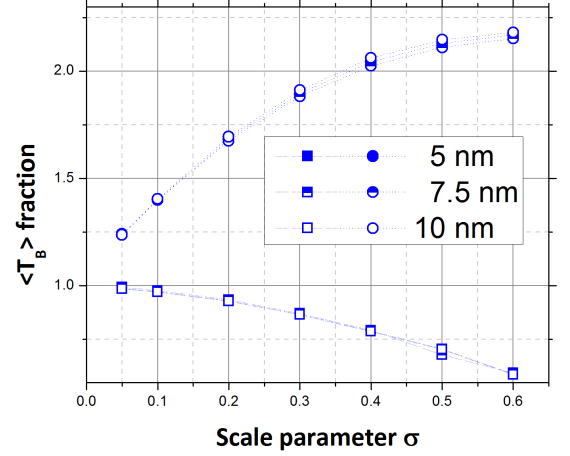


FIG. 8. Values of MAX (circles) and IP (squares) of the simulated curves divided by T_B mean for different MNP radii. The behavior is the same for all sizes.

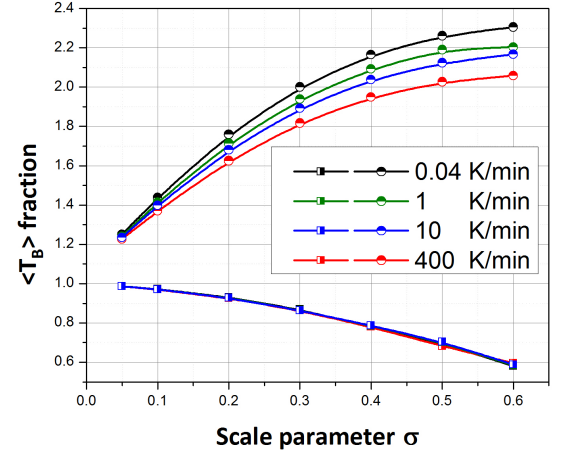


FIG. 9. MAX (circles) and IP (squares) relative to $\langle T_B \rangle$ for 10nm NPM mean radius at different temperature rates.

taken in order to determine the size distribution of the particles (fig 11). A narrow log-normal number diameter distribution ($\text{Ln}N(x)$) was obtained with a 9.54nm mean and a 1.73nm standard deviation. The relative TEM volume distribution was obtained from this results and fitted with a $x\text{Ln}N(x)$ function obtaining a scale parameter $\sigma = 0.55(2)$.

The ZFC-FC routine was carried with a $2.4\text{K}/\text{min}$ rate and a $8\text{kA}/\text{m}$ field on an encapsulated FF sample frozen under a 7T field in order to obtain an ordered system with all the MNP easy axes oriented parallel to the field. The ZFC-FC derivative was calculated and fitted with a $x\text{Ln}N(x)$ distribution using the TEM σ as a fixed parameter with a very good correspondence (figure 12).

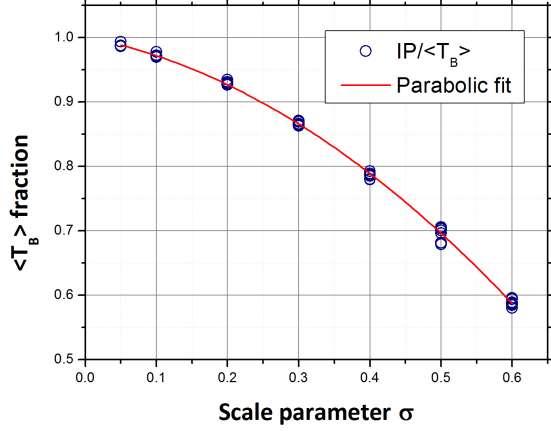


FIG. 10. Parabolic fitting of the universal curve $IP/\langle T_B \rangle$.

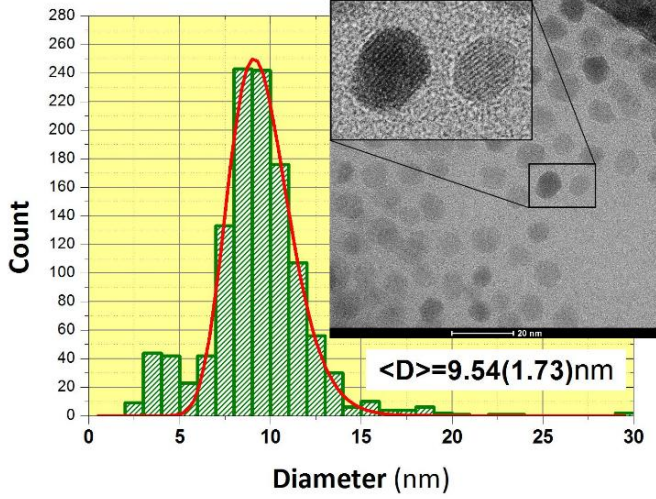


FIG. 11. Size distribution from TEM images. Inset: TEM image example with a magnification showing the crystallinity of the particles.

Figure 13 shows the comparison between T_B distribution obtained from TEM information and the ZFC-FC derivative curve. The translation from TEM volume to T_B was made considering the blocking condition in which the inversion time of the MNPs is approximately equal to the measurement time of the magnetization value:

$$\tau(K, V, h, T) = \tau_0 \exp \left(\frac{KV}{kT_B} (1-h)^2 \right) \approx \tau_m$$

$$\Rightarrow T_B = \frac{KV(1-h)^2}{k \log(\tau_m/\tau_0)}, \quad (12)$$

where $\tau_0 = 1/f_0$ is the inverse of the intrinsic inversion frequency. For a known volume distribution, this comparison can be used to determine the effective K

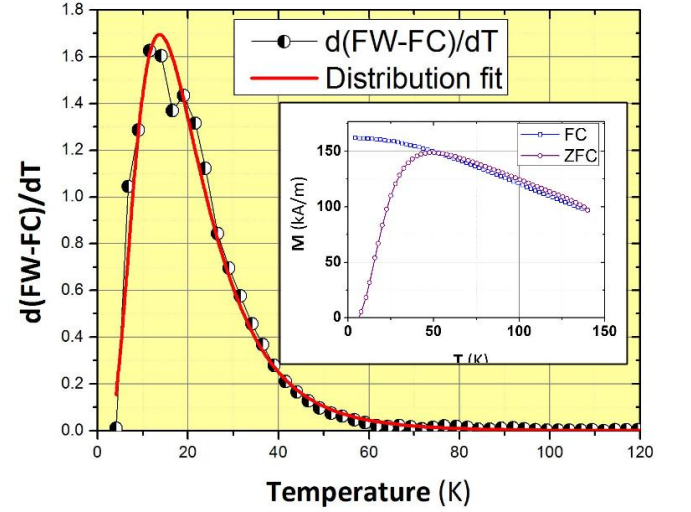


FIG. 12. Log-normal fit on the $d(ZFC-FC)/dT$ derivative. Inset: ZFC and FC experimental curves.

value as the one that maximizes the coincidence between TEM and ZFC-FC distributions. In this case, a value of $34(2)kJ/m^3$ was obtained with a very good correspondence between TEM and ZFC-FC data. This calculation implies some approximations: M_s is considered independent from the temperature in the region of interest, and the relaxation time expression used for the blocking condition 12 considerate only the inversions in the direction of the field. While the first approximation is very reasonably, the blocking condition expression is accurate only in experiments with high $\mu H/(kT)$ ratios, where the reversal frequency are much smaller for the inversions to the antiparallel state.

Additionally, the $IP/\langle T_B \rangle$ ratio was calculated obtaining a value of 0.7(1), compatible with polynomial expression obtained from the simulations.

IV. DISCUSSION AND CONCLUSIONS

The validity of the Micha's method to determine the T_B distribution of non interacting MNPs assembly was demonstrated by numerical simulations and experimental data analysis.

A Stoner-Wolfarth model with thermal agitation was developed in order to simulate the ZFC-FC curves of polysized MNPs assemblies. From this simulation it was clearly demonstrated that the temperature derivative of the ZFC-FC difference is in full coincidence with the T_B distribution of the sample, calculated as the inflection points of each size ZFC curve. Additionally, it came clear from the results that the maximum (MAX) and the inflection point (IP) of the polysized ZFC curve are affected not only by the mean size of the particles, but by the size dispersion. Thus neither IP or MAX are direct

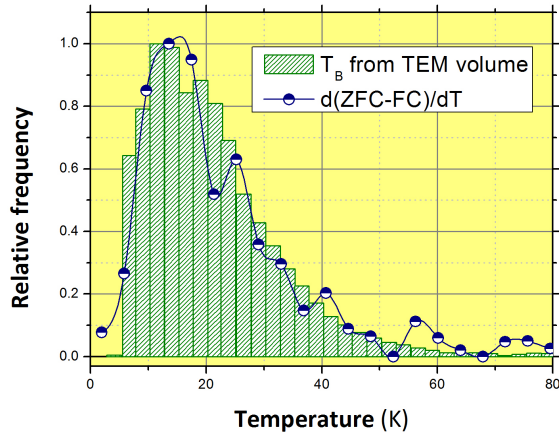


FIG. 13. $d(\text{ZFC-FC})/dT$ derivative together with T_B distribution from TEM volume obtained by fitting K for maximum coincidence.

estimators of the mean T_B . This is an interesting result since these values are commonly used in magnetic characterizations and can lead to estimate T_B values far from the mean. As an example, for a sample with $\sigma = 0.5$ and a heating rate of $4K/min$, $IP = 0.7 < T_B >$ and $MAX = 2.12 < T_B >$. Nevertheless, it was found that the $IP / < T_B >$ ratio depends exclusively on σ , while $MAX / < T_B >$ changes with K and the heating-cooling rate. This behavior reveals a connection between IP , one of the most commonly used T_B criteria and the actual mean value of the blocking temperature. For a sample with known σ , the mean blocking temperature could be obtained from the universal curve presented in this work. This approach of obtaining size distribution information from an universal curve was presented before by Hansen *et al*²² using a rougher model.

In the present development status, the ZFC-FC simulation algorithm does not include a “measurement time” parameter. Just the heating rate is used, so the authors assume that the simulated data points represent the values for “instantaneous” measurements. Therefore, the magnetization values obtained from the simulation won’t be equivalent to the ones obtained in an experiment with the same parameters.

The Micha’s method was then applied to characterize a sample of magnetite nanoparticles coated with oleic acid and suspended in hexane. The volume distribution of the sample was obtained from TEM analysis showing a narrow log-normal shape with a mean diameter of $9.54nm$ and a standard deviation of $1.73nm$. In order to obtain an ordered system, the ferrofluid was frozen under a $7T$ magnetic field. Then, a ZFC-FC routine was carried and a T_B distribution was obtained from the data. This distribution was fitted with a $xLnN[x]$ function using the scale parameter σ obtained from the TEM data as a fixed fitting parameter. The high goodness of the

fitting supports the validity of Micha’s method and the low influence of magnetic interaction between particles which is consistent with the particle to particle distance imposed by the FF concentration. Additionally, the resultant $IP / < T_B >$ values is consistent with the universal curve obtained from the simulations.

Finally, the effective anisotropy constant of the particles was estimated as the value which gives the maximum coincidence between the ZFC-FC T_B distribution and the one obtained from the TEM volume.

The results obtained in this work constitute just a first example of the potential of the presented model in combination with experimental characterization. There is work in progress to enhance the simulation algorithm in order to include the measurement time as a parameter and to considerate both inversions processes in the blocking condition.

- ¹Günter Reiss and Andreas Hütten. Magnetic nanoparticles: Applications beyond data storage. *Nature Materials*, 4(10):725–726, oct 2005.
- ²Quentin A Pankhurst, J Connolly, SK Jones, and JJ Dobson. Applications of magnetic nanoparticles in biomedicine. *Journal of physics D: Applied physics*, 36(13):R167, 2003.
- ³QA Pankhurst, NTK Thanh, SK Jones, and J Dobson. Progress in applications of magnetic nanoparticles in biomedicine. *Journal of Physics D: Applied Physics*, 42(22):224001, 2009.
- ⁴Ronald E Rosensweig. Heating magnetic fluid with alternating magnetic field. *Journal of magnetism and magnetic materials*, 252:370–374, 2002.
- ⁵Magdalena Woińska, Jacek Szczytko, Andrzej Majhofer, Jacek Gosk, Konrad Dziatkowski, and Andrzej Twardowski. Magnetic interactions in an ensemble of cubic nanoparticles: A monte carlo study. *Physical Review B*, 88(14):144421, 2013.
- ⁶Edmund C Stoner and EP Wohlfarth. A mechanism of magnetic hysteresis in heterogeneous alloys. *Philosophical Transactions of the Royal Society of London A: Mathematical, Physical and Engineering Sciences*, 240(826):599–642, 1948.
- ⁷CP Bean and JD Livingston. Superparamagnetism. *Journal of Applied Physics*, 30(4):S120–S129, 1959.
- ⁸Carolin Schmitz-Antoniak. X-ray absorption spectroscopy on magnetic nanoscale systems for modern applications. *Reports on Progress in Physics*, 78(6):062501, 2015.
- ⁹Patricia de la Presa, Yurena Luengo, Victor Velasco, MP Morales, M Iglesias, Sabino Veintemillas-Verdaguer, Patricia Crespo, and Antonio Hernando. Particle interactions in liquid magnetic colloids by zero field cooled measurements: Effects on heating efficiency. *The Journal of Physical Chemistry C*, 119(20):11022–11030, 2015.
- ¹⁰Sandra Sankar, AE Berkowitz, D Dender, JA Borchers, RW Erwin, SR Kline, and David J Smith. Magnetic correlations in non-percolated co-sio 2 granular films. *Journal of magnetism and magnetic materials*, 221(1):1–9, 2000.
- ¹¹F Tournus and A Tamion. Magnetic susceptibility curves of a nanoparticle assembly ii. simulation and analysis of zfc/fc curves in the case of a magnetic anisotropy energy distribution. *Journal of Magnetism and Magnetic Materials*, 323(9):1118–1127, 2011.
- ¹²JS Micha, B Dieny, JR Régnard, JF Jacquot, and J Sort. Estimation of the co nanoparticles size by magnetic measurements in co/sio 2 discontinuous multilayers. *Journal of Magnetism and Magnetic Materials*, 272:E967–E968, 2004.
- ¹³H Mamiya, M Ohnuma, I Nakatani, and T Furubayashim. Extraction of blocking temperature distribution from zero-field-cooled and field-cooled magnetization curves. *IEEE transactions on magnetics*, 41(10):3394–3396, 2005.
- ¹⁴Jing Ju Lu, Huei Li Huang, and Ivo Klik. Field orientations

- and sweep rate effects on magnetic switching of stoner-wohlfarth particles. Journal of applied physics, 76(3):1726–1732, 1994.
- ¹⁵NA Usov and Yu B Grebenshchikov. Hysteresis loops of an assembly of superparamagnetic nanoparticles with uniaxial anisotropy. Journal of Applied Physics, 106(2):023917, 2009.
- ¹⁶Julian Carrey, Boubker Mehdaoui, and Marc Respaud. Simple models for dynamic hysteresis loop calculations of magnetic single-domain nanoparticles: Application to magnetic hyperthermia optimization. Journal of Applied Physics, 109(8):083921, 2011.
- ¹⁷NA Usov. Numerical simulation of field-cooled and zero field-cooled processes for assembly of superparamagnetic nanoparticles with uniaxial anisotropy. Journal of Applied Physics, 109(2):023913, 2011.
- ¹⁸Roger Balian and Dirk Haar. From microphysics to macrophysics: methods and applications of statistical physics, volume 2. Springer Science & Business Media, 2006.
- ¹⁹L Neel. Influence des fluctuations thermiques a l'aimantation des particules ferromagnetiques. Comptes Rendus de l'Académie des Sciences, 228:664–668, 1949.
- ²⁰Amikam Aharoni. Introduction to the Theory of Ferromagnetism, volume 109. Oxford University Press, 2000.
- ²¹Lawrence F Shampine and Mark W Reichelt. The matlab ode suite. SIAM journal on scientific computing, 18(1):1–22, 1997.
- ²²Mikkel Fougth Hansen and Steen Mørup. Estimation of blocking temperatures from zfc/fc curves. Journal of Magnetism and Magnetic Materials, 203(1):214–216, 1999.